OPO OPHTHALMIC AND PHYSIOLOGICAL OPTICS
THE JOURNAL OF THE COLLEGE OF OPTOMETRISTS

Ophthal. Physiol. Opt. 2009 **29:** 256–263

Temporal dynamics of ocular aberrations: monocular vs binocular vision

A. Mira-Agudelo[1,2], L. Lundström[1] and P. Artal[1]

[1]Laboratorio de Óptica, Centro de Investigación en Óptica y Nanofísica (CiOyN), Universidad de Murcia, Campus de Espinardo Murcia, Murcia 30100, Spain, and [2]Grupo de Óptica y Fotónica, Instituto de Fisica, Universidad de Antioquia, Medellín, Antioquia, Colombia

Abstract

The temporal dynamics of ocular aberrations are important for the evaluation of, e.g. the accuracy of aberration estimates, the correlation to visual performance, and the requirements for real-time correction with adaptive optics. Traditionally, studies on the eye's dynamic behavior have been performed monocularly, which might have affected the results. In this study we measured aberrations and their temporal dynamics both monocularly and binocularly in the relaxed and accommodated state for six healthy subjects. Temporal frequencies up to 100 Hz were measured with a fast-acquisition Hartmann–Shack wavefront sensor having an open field-of-view configuration which allowed fixation to real targets. Wavefront aberrations were collected in temporal series of 5 s duration during binocular and monocular vision with fixation targets at 5 m and 25 cm distance. As expected, a larger temporal variability was found in the root-mean-square wavefront error when the eye accommodated, mainly for frequencies lower than 30 Hz. A statistically-significant difference in temporal behavior between monocular and binocular viewing conditions was found. However, on average it was too small to be of practical importance, although some subjects showed a notably higher variability for the monocular case during near vision. We did find differences in pupil size with mono- and binocular vision but the pupil size temporal dynamics did not behave in the same way as the aberrations' dynamics.

Keywords: accommodation, binocular vision, eye's temporal dynamics, ocular aberrations, pupillary oscillations

Introduction

The eye is a dynamic optical system with aberrations that vary due to many different factors at temporal scales ranging from fractions of a second (Hofer *et al*., 2001a) to years (Artal *et al*., 1993). Knowledge of this temporal behaviour is important for the evaluation of, for example, its impact on accurate estimates of ocular aberrations, the relationship between dynamics and visual performance, and the implications for real-time correction using adaptive optics (Prieto *et al*., 2000; Fernández *et al*., 2001; Hofer *et al*., 2001b; Diaz-Santana *et al*., 2003; Day *et al*., 2006; Hampson *et al*., 2006; Zhu *et al*., 2006).

Since the early work of Collins (1937), the short-term fluctuations of the ocular aberrations have been studied by many investigators, who have found instabilities as large as a quarter of a diopter in steady-state accommodation (Campbell *et al*., 1959; Charman and Heron, 1988; Winn and Gilmartin, 1992; Hofer *et al*., 2001a; Zhu *et al*., 2004). Arnulf *et al*. (1981) used a binocular real-time double-pass instrument (Santamaría *et al*., 1987) to demonstrate the fast temporal changes of the eye's optics. Although the major fluctuations are found in defocus, almost all other low- and high-order aberrations have been shown to exhibit temporal instability, with similar spectra and frequency components (Hofer *et al*., 2001a; Nirmaier *et al*., 2003; Zhu *et al*., 2004, 2006). The properties of these variations are affected by changes in the accommodative state and the

Received: 4 November 2008
Revised form: 15 January 2009
Accepted: 22 January 2009

Correspondence and reprint request to: A. Mira-Agudelo.
Tel.: +34 968398549; Fax: +34 968363528.
E-mail address: amira@um.es

doi: 10.1111/j.1475-1313.2009.00655.x

rhythm of the cardiopulmonary system (Hampson *et al*., 2005). It has also been proposed that they can be affected by whether the subject uses monocular or binocular fixation (Campbell, 1960; Krueger, 1978; Charman and Heron, 1988; Flitcroft *et al*., 1992). On the other hand, the effect of correcting aberrations on the accommodation response has also been evaluated in a previous work (Fernández and Artal, 2005).

Changes in accommodation are known not only to affect the dynamics of the ocular aberrations but also to be associated with concurrent variations in pupil size (Kasthurirangan and Glasser, 2005). A similar relation could be proposed between the variations in the dynamics of the ocular aberrations and the changes in pupil diameter related to monocular or binocular viewing conditions. Previous studies have shown that the pupil size is significantly smaller under binocular compared to monocular viewing (Boxer Wachler, 2003; Kawamorita and Uozato, 2006).

The quantification of the possible differences between measurements performed either monocularly or binocularly is relevant to determine which of these two viewing conditions should be preferred in experimental studies. Recently, Seidel *et al*. (2005) and Chin *et al*. (2008) have found some, but not statistically significant, differences between monocular and binocular viewing in static aberrations and their variations. However, Seidel *et al*. performed measurements as fast as 102.4 Hz for six accommodation states but only recorded the refraction of the eye. Chin *et al*. obtained low- and higher-order aberrations of the eye but only for one accommodation state ($\sim$ 0.4 D) and with a temporal sampling frequency of 20.5 Hz.

The present study explores the possible impact on the ocular aberrations and their temporal dynamics of using monocular or binocular fixation. The aberrations were measured with a Hartmann–Shack (HS) wavefront sensor operating at a rate of 200 Hz. The system records HS images from one eye at a time within an open field-of-view configuration, which allows binocular or monocular fixation on real targets at near and far. The variation in pupil size is also estimated from the HS images, and is used to investigate relations between the dynamics of the pupil and the aberrations of the eye.

Methods

The ocular wavefront aberrations and their temporal changes were assessed with a laboratory Hartmann–Shack (HS) wavefront sensor, which is described in detail in *Figure 1* (see e.g. Prieto *et al*., 2000 for additional information on the principle). The sensor was built with an open field-of-view configuration to allow either binocular or monocular fixation to different distances with natural accommodation and vergence. A

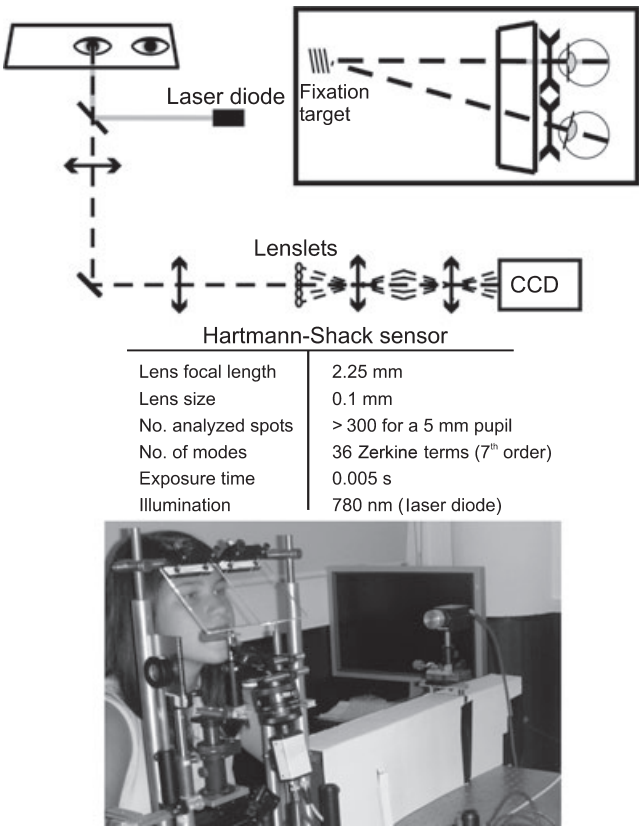

Figure 1. Schematic drawing, data, and photo of the open field wavefront sensor. The subject views the fixation targets through a large hot mirror and the rest of the sensor is located below and to the side of the subject so as not to disturb the field-of-view. The inset shows the set-up from above during a binocular accommodation measurement with spectacles.

bite-bar was used to stabilize the head of the subject while he or she was viewing the target through a large hot mirror, which transmitted visible light, and reflected the infrared measurement light into the eye, and the emerging wavefront back to the sensor. Apart from the hot mirror, the other key elements are a high density lenslet array (10 microlenses per millimeter, 2.25 mm focal length) and a high speed CCD camera (Jai-Pulnix TM 6745cl) recording 200 frames per second, with a resolution of 640 $\times$ 480 pixels. The sensor was designed with a magnification of 0.4 to allow pupil diameters of up to 8 mm to be imaged on to the 1/3″-chip of the CCD-camera. It must be noted that this system allows binocular fixation, but that it only measures on one eye at a time.

The right eyes of six young (age range from 25 to 31 years) healthy subjects were measured; three emmetropes (spherical refractive error between $\pm$ 0.5 D and maximum astigmatism of -0.5 D) and three myopes (spherical refractive error between -3.5 and -2.75 D and maximum astigmatism of -0.75 D). No cycloplegia was used and the background illumination in the room

was low, to achieve naturally large pupils. The study followed the ethical principles of the Declaration of Helsinki.

Four different series of measurement were performed. The wavefront aberrations of the right eye were measured with a fixation target placed at 5 m distance (0.2 D) and with a target at 25 cm distance, i.e. accommodation of 4.0 D. For each fixation distance, the subject was instructed to first fixate using both eyes and then the left eye was blocked to achieve monocular fixation to the same target. The fixation target was a pattern which consists of groups of three bars with dimensions from large to small (USAF 1951 Test Chart; JML Optical Industries, Rochester, NY, USA). To allow the same fixation target to be used by all subjects, myopes were measured with their spectacle correction in place. The disadvantage of using negative spectacles is that the eye will accommodate slightly less with the spectacles in place: whereas the emmetropic subjects experienced a 4.0 D accommodation-stimulus, the myopic subjects with spectacles experienced approximately 3.5 D.

For each subject and case, 10 videos of 1000 frames each (5 s) was recorded. Each series of wavefront aberrations was fitted with Zernike polynomials (American National Standards Institute, 2004) up to 7th order over the central 5 mm circular zone of the pupil. Besides the variation of these Zernike coefficients, the evolution of the total root-mean-square (RMS) wavefront error of each video frame was also calculated and the temporal power spectrum of the RMS error sequence was computed using a discrete fast Fourier transform algorithm from Matlab® software (The Mathworks Inc., Boston, MA, USA). Because of the 5 s duration and 200 Hz sampling rate of the videos, the frequency range for the power spectra was between 0.2 and 100 Hz.

The HS spot patterns were also used to indirectly measure the size of the pupil by using the contouring spots in each frame of the recorded HS videos (see *Figure 2*). Although this pupil size estimate is affected by ocular aberrations (through the position of the spots) and by the pitch of the lenslet array (0.1 mm in this setup, which corresponds to 0.25 mm in the pupil plane), it provides a good relative measure of the dynamic variations in pupil size at the same moment that the aberrations were measured.

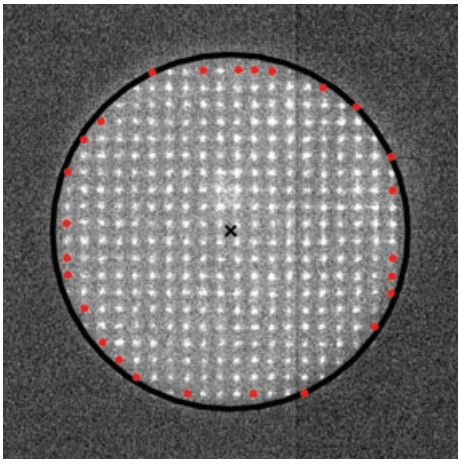

Figure 2. Indirect measurement of the size of the pupil by using the contouring spots (red points) of the HS images. The black circle is the smallest possible that contains all spots and its diameter is an estimation of the pupil size. The original contrast of the image was changed to show the edge of the pupil clearly.

Results

The wavefront aberrations were assessed in ten videos for each subject and measurement case, i.e. binocular/monocular and far/near fixation. However, because of blinking, subjects AD and LL only had nine videos. Zernike polynomials for each frame were processed in two ways: first, the coefficients were averaged over each video to compare the change in the static amount of aberrations between the four different measurement cases; and secondly, the variation of the root-mean-square (RMS) error within each video, i.e. the temporal dynamics of the aberrations, was analyzed by the power spectrum.

Figure 3 shows an example of the outcome of the measurements for subject LL: the four wavefront maps are the average of all frames in all videos for each case of monocular and binocular fixation to far and near targets. As can be seen, the measurements exhibit the expected difference in defocus between far and near viewing, but the binocular and monocular cases are similar. The same trends were seen also for the other subjects when the average Zernike coefficients for the four cases were compared.

Figure 4 shows the averaged difference in the Zernike coefficients between the unaccommodated (0.2 D) and the accommodated (4.0 D) state of the six subjects for binocular fixation (the results for monocular fixation are not shown because they were very similar). The error bars represent the standard deviation of the differences as calculated from the distribution of the 10 mean values for each case and subject. The largest changes in the ocular aberrations terms occurred in defocus (term Z4 with a mean difference of 2.22 ± 0.03 μm), coma term Z7, spherical aberration (Z12) and astigmatism term Z5. These last three terms got smaller with accommodation, on average by 0.09 ± 0.01, 0.064 ± 0.007, and 0.06 ± 0.02 μm, respectively. An analysis of variance test (ANOVA, $p < 0.01$) showed significant differences with accommodation for both the binocular and the monocular case in all 2nd, 3rd, and 4th order coefficients except for the coma term Z8 and the trefoil term Z9.

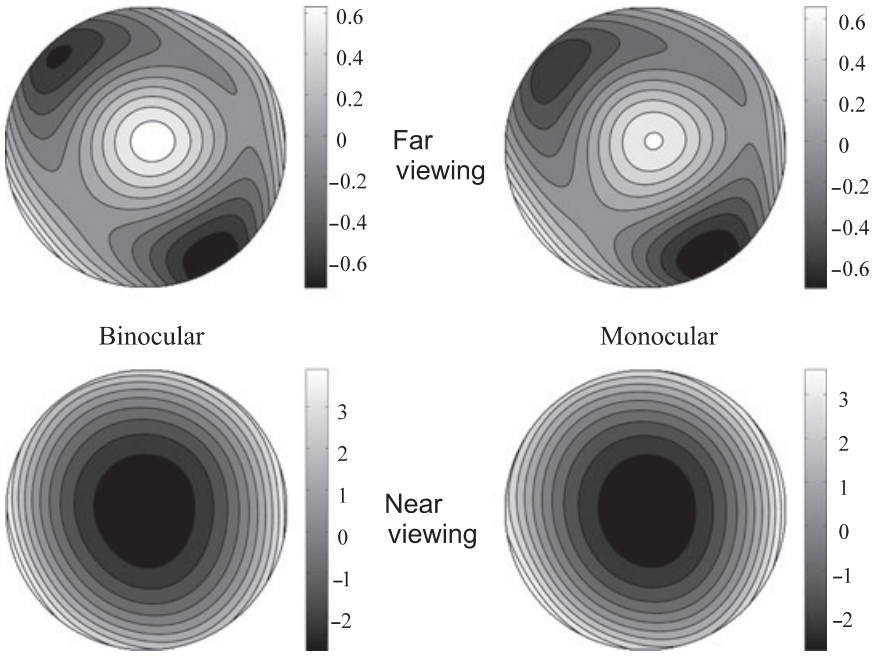

Figure 3. Averaged wavefront map comparison for the four studied cases in the right myopic eye of subject LL, calculated for a 5.0 mm pupil diameter. Scale in μm.

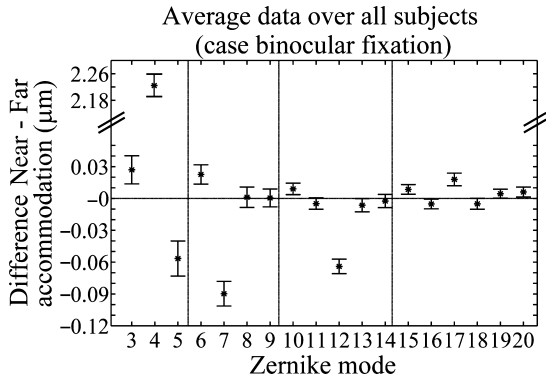

Figure 4. Averaged differences in Zernike coefficients (up to 5th order) between near (4 D) and far (0.2 D) fixation with binocular viewing for the six subjects of this study. Data are calculated from the mean values of the videos for each case. Error bars are ± 1 S.D. (Zernike modes in standard OSA). Vertical bars separate successive radial orders.

The comparison between the monocular and binocular viewing conditions is shown for both accommodation states in *Figure 5*. The largest difference was in defocus, with 0.06 μm for far vision and 0.1 μm for near, i.e. somewhat more accommodation for the monocular case (approximately 0.07 and 0.11 D). Other significant, but small, differences were found for astigmatism (Z3 and Z5), for one trefoil term (Z9), and for quadrifoil (Z10 and Z14) (ANOVA, $p < 0.01$). The changes in these averaged aberrations between monocular and binocular fixation were not significantly dependent on the state of accommodation.

To analyze the temporal dynamics of the wavefront aberrations, the total RMS wavefront error of each frame was calculated from the Zernike coefficients over the 5 mm pupil and Fourier transformed with respect to time to give the temporal power spectrum. The 10

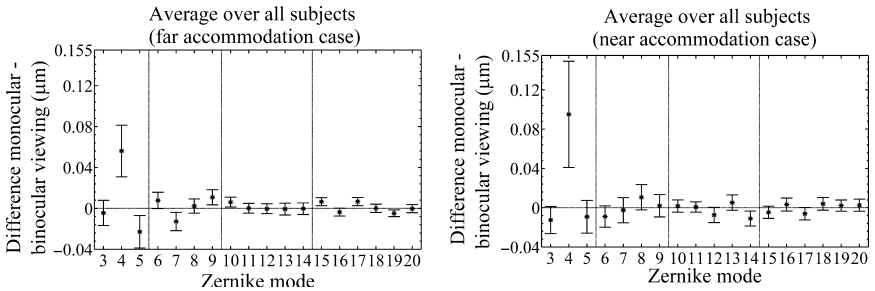

Figure 5. Averaged differences in Zernike coefficients (up to 5th order) between monocular and binocular viewing for the six subjects of this study. Left graph shows the unaccommodated case and the right graph shows the differences during accommodation. Data are calculated from the mean values of the videos for each case. Error bars are ± 1 S.D. (Zernike modes in standard OSA). Vertical bars separate successive radial orders.

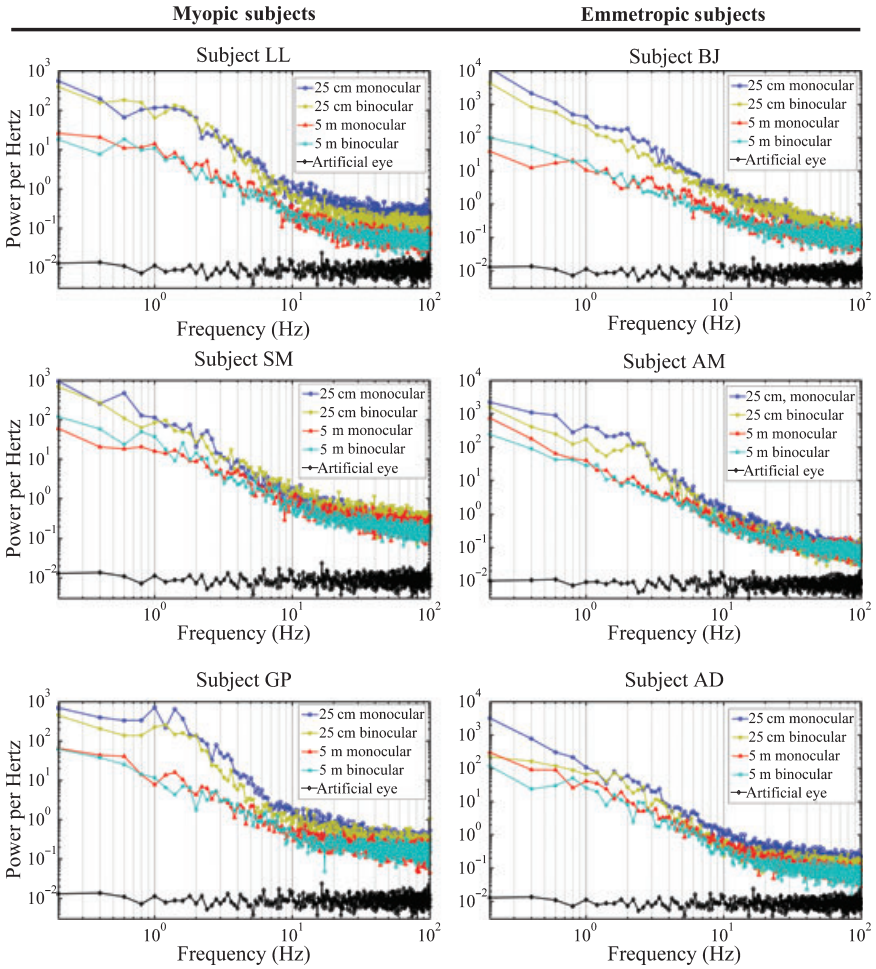

Figure 6. Comparison of the averaged power spectra in four studied cases for the 6 subjects of this study. The power spectra show the fluctuations over 5 s in total RMS wavefront error; the horizontal axes give the time frequencies of the variations and the values on the vertical axes represent how conspicuous that frequency is in the variation of the RMS. The off-set value represented for a static artificial eye is also shown. Note that the axes are logarithmic.

spectra achieved for each subject and measurement case were then averaged to produce the mean RMS power spectra of *Figure 6*. Here, the mean power spectra of each subject and case are shown together with the off-set value, or the sensor's noise level, which was calculated from the fluctuations in measured RMS error of an artificial eye. Although there are individual differences (compare, e.g. the myopic subject LL and the emmetrope subject BJ: BJ has a larger difference for the monocular vs binocular viewing in the low and middle frequency ranges) some general trends can also be distinguished.

For all subjects a clear difference between the far and near fixation case can be seen; the unaccommodated cases have lower power and a frequency decay of 4 dB per octave up to 30 Hz, whereas the near accommodation cases have higher power with a decay of 5.5 dB per octave. This means that the slower (low frequency) variations in the ocular aberrations are larger when the eye accommodates, and that the faster variations (frequency higher than 30 Hz) are present in equal amounts both with and without accommodation.

The differences in the dynamical fluctuations of ocular aberrations between far and near vision were similar for both the monocular and binocular viewing conditions. As shown in *Figure 6*, the power spectra for the two conditions of monocular and binocular fixation were quite alike, although some subjects showed a slightly higher variability for the monocular case during near vision. To quantify these differences, the area under each power spectrum graph was calculated for three temporal frequency ranges: [0.2–1.4 Hz], [1.4–12.4 Hz] and [12.4–100 Hz]. *Figure 7* compares the areas averaged over the six subjects and shows that there is a significant difference for the monocular vs binocular viewing in the low and middle frequency ranges for the accommodated state (ANOVA, $p < 0.01$). The same trend, but smaller, can also be discerned for

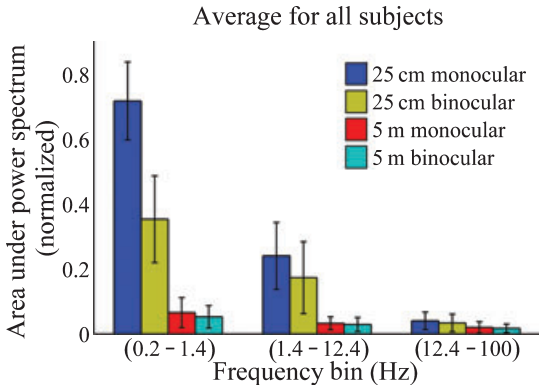

Figure 7. Distribution of area under curve for three different temporal frequency bins in the RMS power spectra, averaged over all subjects for the studied cases. Error bars are ± 1 S.D. Data are normalized to the largest total area.

Table 1. Differences between monocular and binocular relative pupil diameter for accommodated and unaccommodated states

Subject	Near accommodation*	Far accommodation*
LL	0.5 ± 0.2	0.7 ± 0.2
SM	0.9 ± 0.2	0.9 ± 0.2
GP	1.0 ± 0.2	0.8 ± 0.1
BJ	0.6 ± 0.4	0.4 ± 0.2
AM	0.1 ± 0.1	1.1 ± 0.3
AD	0.8 ± 0.2	1.0 ± 0.2
Average	0.6 ± 0.3	0.8 ± 0.3

*Mean differences ± S.E. in millimeter

the unaccommodated state and for the highest frequencies.

The pupil sizes estimated from the HS videos were processed in a similar way to the Zernike coefficients, i.e. average values and mean power spectra were calculated for each case and subject.

Table 1 shows the difference in relative pupil diameter between the monocular and the binocular case for near and far accommodation for each subject, with average values of 0.6 ± 0.3 and 0.8 ± 0.3 mm respectively.

The power spectra in *Figure 8* show the dynamics of the size of the pupil for two subjects in the same manner as in *Figure 6* for aberrations. The general behavior of all pupil power spectra was very similar for almost all subjects and cases, with a 5 dB decay per octave up to a frequency of 20 Hz. This slope is different from those found in the ocular aberration power spectra and no clear difference was found between the accommodation states (the corresponding falls for the aberrations were 4 dB per octave for far and 5.5 dB per octave for near, both for frequencies below 30 Hz). An analysis of the areas under the pupil power spectrum curves is shown in *Figure 9*; there was a high inter-subject variability and the relative differences between the four studied cases in the aberrations dynamics can not be seen here.

Discussion

The differences between near and far accommodation found here coincide well with previous studies. The decrease in the static mean values of coma (Z7), spherical aberration (Z12), and astigmatism (Z5) with accommodation has previously been reported (López-Gil *et al.*, 1998; He *et al.*, 2000; Artal *et al.*, 2002; Cheng *et al.*, 2004). Also the increase in the dynamics of the ocular aberrations with accommodation (power spectrum slope of 5.5 dB instead of 4 dB per octave) have been found earlier (Denieul, 1982; Miege and Denieul, 1988; Hofer *et al.*, 2001a; Day *et al.*, 2006; Zhu *et al.*, 2006).

Generally, the measured wavefronts showed a similar behavior both for the binocular and the monocular case and the average differences in the static aberrations were small. However, the changes in the dynamic variation were subject and accommodation dependent, with a higher variability for the monocular case during near vision, especially for frequencies lower than 12.4 Hz. This difference is in agreement with the hypothesis of Campbell (1960), who suggested that accommodation fluctuations could be of 'greater magnitude (…for a monocular fixation) due to the absence of the convergence-fixation reflex'. Other recent studies have investigated the same hypothesis without finding a statistically significant difference between monocular

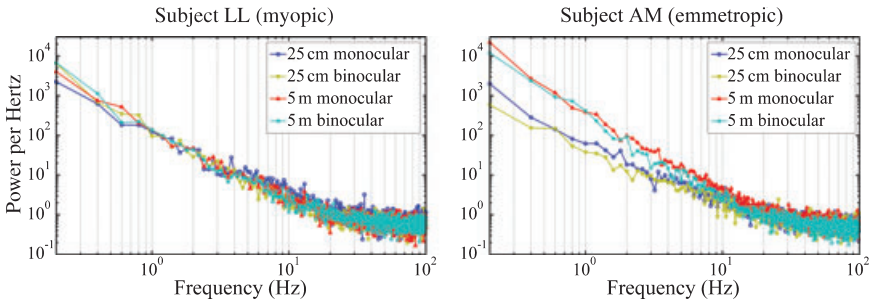

Figure 8. Comparison of the averaged pupil power spectra in four studied cases for one myopic (left) and one emmetropic subject (right). The mean power spectra show the fluctuations over 5 s in the estimated pupil size. Note that the axes are logarithmic.

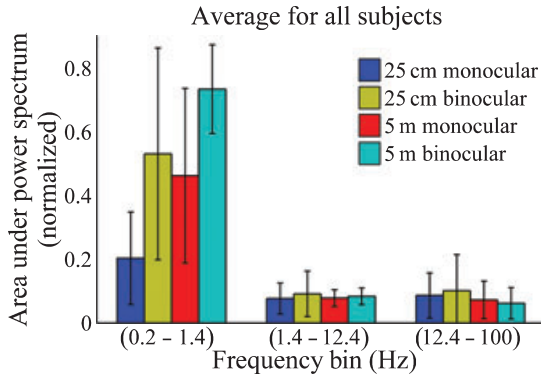

Figure 9. Distribution of area under curve for three different temporal frequency bins in the pupil power spectra, averaged over all subjects for the studied cases. Error bars are ± 1 S.D. Data are normalized to the largest total area.

and binocular fixation (Seidel *et al*., 2005; Chin *et al*., 2008), maybe because the optometer used by Seidel *et al*. to record the refractive error of the eye had a resolution of only 0.12 D and Chin *et al*. had the fixation target placed further away.

The pupil size increased with monocular fixation as found previously (e.g. Boxer Wachler, 2003). Although the power spectra of the pupil size (Mclaren *et al*., 1992; Rosenberg and Kroll, 1999) and the power spectra of the aberrations show a similar (but not the same) fast logarithmic decay (linear in the log-log plots of *Figures 6 and 8*) for frequencies below 30 Hz, the relative differences in the pupil size dynamics between the studied cases did not exhibit any general trend nor did it show an apparent relation with those from the power spectra of the aberrations. These relative comparisons should be valid even though the method to estimate the size of the pupil was indirect. However, the measured size could be influenced by the shape of the wavefront, especially defocus, which is the reason why the pupil sizes for far and near accommodation were not compared.

An important issue for this study is if the outcome of the aberration measurements is independent of whether the subject is using monocular or binocular fixation. The differences we found in static averaged aberrations are too small to be of practical importance, when the eye was both relaxed and accommodated. Also the dynamics of the RMS error were similar using one and two eyes to fixate objects at large distances. However, for near tasks the fluctuations seem to increase. This implies that binocular fixation during high-temporal-resolution measurements could be needed for a correct assessment of the natural dynamics in the accommodated state. In this context, it is important to note that the monocular fixation which has been evaluated here is to a real target, i.e. the same conclusion might not apply to targets seen through e.g. Badal optometers (Seidel *et al*., 2005).

Conclusion

In this study the mean values and the dynamic variations of the ocular aberrations have been measured on the right eye of six subjects. A HS wavefront sensor with an open field-of-view was used to compare the ocular optics for monocular and binocular fixation in one unaccommodated and one accommodated state (0.2 and 4.0 D). The mean values and dynamics of the pupil were also estimated from the HS spot pattern. The comparisons showed the expected difference between the accommodative states both in the static and the dynamic aberrations. The monocular and binocular viewing conditions were also similar, although some differences in the dynamics were noted during accommodation. The corresponding difference in pupil size dynamics was not found. We therefore conclude that ocular aberrations and their dynamics can be reliably measured under monocular viewing to a real fixation target.

Acknowledgements

This research was supported in part by 'Ministerio de Educación y Ciencia', Spain (grant FIS2007-64765), 'Fundación Séneca', Murcia (04524/GERM/06) and EU-Marie Curie Research Training Network MY EUROPIA (MRTN-CT-2006-034021). Alejandro Mira-Agudelo acknowledges the financial support from 'COLCIENCIAS' Colombia and 'Universidad de Antioquia' Colombia.

References

American National Standards Institute (2004). *Methods for Reporting Optical Aberrations of Eyes*, Optical Laboratories Association, Merriefield, ANSI Z80 28-2004.

Arnulf, A., Santamaría, J. and Bescós, J. (1981) A cinematographic method for the dynamic study of the image-formation by the human-eye – microfluctuations of the accommodation. *J. Optics (Paris)* **12,** 123–128.

Artal, P., Ferro, M., Miranda, I. and Navarro, R. (1993) Effects of aging in retinal image quality. *J. Opt. Soc. Am. A* **10,** 1656–1662.

Artal, P., Fernández, E. J. and Manzanera, S. (2002) Are optical aberrations during accommodation a significant problem for refractive surgery? *J. Refractive Surg.* **18,** S563–S566.

Boxer Wachler, B. S. (2003) Effect of pupil size on visual function under monocular and binocular conditions in LASIK and non-LASIK patients. *J. Cataract Refract. Surg.* **29,** 275–278.

Campbell, F. W. (1960) Correlation of accommodation between the 2 eyes. *J. Opt. Soc. Am.* **50,** 738–738.

Campbell, F. W., Robson, J. G. and Westheimer, G. (1959) Fluctuations of accommodation under steady viewing conditions. *J. Physiol.* **145,** 579–594.

Charman, W. N. and Heron, G. (1988) Fluctuations in accommodation – a review. *Ophthalmic Physiol. Opt.* **8,** 153–164.

Cheng, H., Barnett, J. K., Vilupuru, A. S., Marsack, J. D., Kasthurirangan, S., Applegate, R. A. and Roorda, A. (2004) A population study on changes in wave aberrations with accommodation. *J. Vision* **4,** 272–280.

Chin, S. S., Hampson, K. M. and Mallen, E. A. H. (2008) Binocular correlation of ocular aberration dynamics. *Opt. Express* **16,** 14731–14745.

Collins, G. (1937) The electronic refractometer. *Br. J. Physiol. Opt.* **1,** 30–40.

Day, M., Strang, N. C., Seidel, D., Gray, L. S. and Mallen, E. A. H. (2006) Refractive group differences in accommodation microfluctuations with changing accommodation stimulus. *Ophthalmic Physiol. Opt.* **26,** 88–96.

Denieul, P. (1982) Effects of stimulus vergence on mean accommodation response, micro-fluctuations of accommodation and optical-quality of the human-eye. *Vision Res.* **22,** 561–569.

Diaz-Santana, L., Torti, C., Munro, I., Gasson, P. and Dainty, C. (2003) Benefit of higher closed-loop bandwidths in ocular adaptive optics. *Opt. Express* **11,** 2597–2605.

Fernández, E. J. and Artal, P. (2005) Study on the effects of monochromatic aberrations in the accommodation response by using adaptive optics. *J. Opt. Soc. Am. A* **22,** 1732–1738.

Fernández, E. J., Iglesias, I. and Artal, P. (2001) Closed-loop adaptive optics in the human eye. *Opt. Lett.* **26,** 746–748.

Flitcroft, D. I., Judge, S. J. and Morley, J. W. (1992) Binocular interactions in accommodation control – effects of anisometropic stimuli. *J. Neurosci.* **12,** 188–203.

Hampson, K. M., Munro, I., Paterson, C. and Dainty, C. (2005) Weak correlation between the aberration dynamics of the human eye and the cardiopulmonary system. *J. Opt. Soc. Am. A* **22,** 1241–1250.

Hampson, K. M., Paterson, C., Dainty, C. and Mallen, E. A. H. (2006) Adaptive optics system for investigation of the effect of the aberration dynamics of the human eye on steady-state accommodation control. *J. Opt. Soc. Am. A* **23,** 1082–1088.

He, J. C., Burns, S. A. and Marcos, S. (2000) Monochromatic aberrations in the accommodated human eye. *Vision Res.* **40,** 41–48.

Hofer, H., Artal, P., Singer, B., Aragon, J. L. and Williams, D. R. (2001a) Dynamics of the eye's wave aberration. *J. Opt. Soc. Am. A* **18,** 497–506.

Hofer, H., Chen, L., Yoon, G. Y., Singer, B., Yamauchi, Y. and Williams, D. R. (2001b) Improvement in retinal image quality with dynamic correction of the eye's aberrations. *Opt. Express* **8,** 631–643.

Kasthurirangan, S. and Glasser, A. (2005) Characteristics of pupil responses during far-to-near and near-to-far accommodation. *Ophthalmic Physiol. Opt.* **25,** 328–339.

Kawamorita, T. and Uozato, H. (2006) Changes of natural pupil size and ocular wavefront aberrations under the binocular and the monocular conditions. *J. Vision* **6,** 54–54.

Krueger, H. (1978) Fluctuations in accomodation of human eye to monocular and binocular fixation. *Albrecht Von Graefes Arch. Klin. Exp. Ophthalmol.* **205,** 129–133.

López-Gil, N., Iglesias, I. and Artal, P. (1998) Retinal image quality in the human eye as a function of the accommodation. *Vision Res.* **38,** 2897–2907.

Mclaren, J. W., Erie, J. C. and Brubaker, R. F. (1992) Computerized analysis of pupillograms in studies of alertness. *Invest. Ophthalmol. Vis. Sci.* **33,** 671–676.

Miege, C. and Denieul, P. (1988) Mean response and oscillations of accommodation for various stimulus vergences in relation to accommodation feedback-control. *Ophthalmic Physiol. Opt.* **8,** 165–171.

Nirmaier, T., Pudasaini, G. and Bille, J. (2003) Very fast wavefront measurements at the human eye with a custom CMOS-based Hartmann–Shack sensor. *Opt. Express* **11,** 2704–2716.

Prieto, P. M., Vargas-Martin, F., Goelz, S. and Artal, P. (2000) Analysis of the performance of the Hartmann–Shack sensor in the human eye. *J. Opt. Soc. Am. A* **17,** 1388–1398.

Rosenberg, M. L. and Kroll, M. H. (1999) Pupillary hippus: an unrecognized example of biologic chaos. *J. Biol. Syst.* **7,** 85–94.

Santamaría, J., Artal, P. and Bescós, J. (1987) Determination of the point-spread function of human eyes using a hybrid optical-digital method. *J. Opt. Soc. Am. A* **4,** 1109–1114.

Seidel, D., Gray, L. S. and Heron, G. (2005) The effect of monocular and binocular viewing on the accommodation response to real targets in emmetropia and myopia. *Optom. Vis. Sci.* **82,** 279–285.

Winn, B. and Gilmartin, B. (1992) Current perspective on microfluctuations of accommodation. *Ophthalmic Physiol. Opt.* **12,** 252–256.

Zhu, M. X., Collins, M. J. and Iskander, D. R. (2004) Microfluctuations of wavefront aberrations of the eye. *Ophthalmic Physiol. Opt.* **24,** 562–571.

Zhu, M. X., Collins, M. J. and Iskander, D. R. (2006) The contribution of accommodation and the ocular surface to the microfluctuations of wavefront aberrations of the eye. *Ophthalmic Physiol. Opt.* **26,** 439–446.